Journal of Catalysis 279 (2011) 389–396

Contents lists available at ScienceDirect

Journal of Catalysis

journal homepage: www.elsevier.com/locate/jcat

Hydrodechlorination of chloromethanes with a highly stable Pt on activated carbon catalyst

M.A. Álvarez-Montero [a], L.M. Gómez-Sainero [a,*], A. Mayoral [b], I. Diaz [c], R.T. Baker [d], J.J. Rodriguez [a]

[a] Área de Ingeniería Química, Facultad de Ciencias, Universidad Autónoma de Madrid, Cantoblanco, 28049 Madrid, Spain
[b] Laboratorio de Microscopía Avanzada, Instituto de Nanociencia de Aragón, Universidad de Zaragoza, 50018 Zaragoza, Spain
[c] Instituto de Catálisis y Petroleoquímica, CSIC, 28049 Madrid, Spain
[d] East Chem, School of Chemistry, University of St Andrews, North Haugh, St Andrews, Fife, KY16 9ST, UK

ARTICLE INFO

Article history:
Received 11 February 2011
Revised 21 February 2011
Accepted 23 February 2011

Keywords:
Hydrodechlorination
Residual gases
Dichloromethane
Chloroform
Pt/activated carbon catalyst

ABSTRACT

A platinum catalyst with activated carbon-support (Pt/C) was prepared and showed a high activity for the deep gas-phase hydrodechlorination (HDC) of dichloromethane (DCM) and chloroform (TCM), with conversions of up to 70% and 100%, respectively (operating conditions: atmospheric pressure, reaction temperatures of 150–250 °C, and space–times of 0.08–1.7 kg h mol^{-1}). The catalyst was highly selective to methane (the only non-chlorinated product) with selectivities of up to 85% for HDC of DCM and 93% for HDC of TCM. The catalyst showed exceptional stability with no loss of activity after 26 days on stream in the HDC of DCM. This can be ascribed to its high resistance to poisoning by organic compounds compared to Pd/C catalysts previously studied. This can be attributed to re-dispersion of Pt during the reaction and to the high proportion of metal in the zero-valent state (Pt^0) which disfavors the stabilization of chlorocarbon compounds at the active centers of the catalyst.

1. Introduction

The release of chloromethanes to the atmosphere constitutes a significant environmental problem. These compounds have harmful effects on human health and their emission contributes to the destruction of the ozone layer, to global warming and to photochemical smog formation [1–3]. In particular, dichloromethane (DCM) and chloroform (TCM) are included in the list of the 17 highly dangerous chemicals targeted in the emissions reduction effort (33/50 Program) of the US Environmental Protection Agency (EPA). Despite their high toxicity, DCM and TCM are widely used in industry. Because of their particular properties (high stability, low flammability, and solvent properties) suitable substitutes for many of their applications have still not been developed. In consequence, the chloromethanes are some of the most common chlorinated compounds in residual gas streams. Their emission is submitted to progressively more stringent regulations, and development of suitable technologies for the treatment of these compounds has become necessary. Catalytic hydrodechlorination shows potential economic and environmental advantages when compared with other techniques and is a subject of growing interest. Incineration has high energy requirements and can generate even more toxic compounds than the original chlorocarbon, such as dioxins and furans [4–6]. Catalytic combustion is less energetically demanding but does not avoid the contamination problem completely [6,7]. Treatments based on photochemical, biotechnological or electrochemical processes result in low conversion or difficult scale-up [8–10].

A growing bibliography is devoted to the hydrodechlorination of organochlorinated compounds by catalysts based on different metals and supports, including some reviews focused on the chemistry of catalytic dehalogenation of chlorocarbons and chlorofluorocarbons [11,12]. Nevertheless, little attention is paid to hydrodechlorination of chloromethanes other than carbon tetrachloride (TTCM), probably due to their lower reactivity (the reactivity of chloromethanes decreases in the order TTCM > TCM > DCM > MCM [13,14]). Moreover, in the few studies devoted to the gas-phase, deep hydrodechlorination of chloroform and dichloromethane with metal supported catalysts either a rapid deactivation has been reported or long-term experiments were not performed [13,15–24]. To the best of our knowledge, catalysts which do not suffer significant deactivation in the hydrodechlorination of chloromethanes after more than two days on stream have not so far been reported, which is a limiting issue for the application of this technology. In the growing number of studies dealing with the causes of deactivation of the catalysts in hydrodechlorination reactions, this phenomenon has been attributed to poisoning by HCl and chlorine species, coke formation (in some cases including chlorine in its composition), loss of metal through the

* Corresponding author. Address: Ingeniería Química, Facultad de Ciencias, Universidad Autónoma de Madrid, Cantoblanco, 28049 Madrid, Spain. Fax: +34 914973516.
E-mail address: luisa.gomez@uam.es (L.M. Gómez-Sainero).

0021-9517/$ - see front matter © 2011 Elsevier Inc. All rights reserved.
doi:10.1016/j.jcat.2011.02.009

formation of volatile compounds and metal sintering, depending on the catalyst components, changes in the oxidation state of metal and metal migration [21,25–31]. Pt is commonly reported to be less active than Pd but shows a better stability [32,33,28,29]. The support also plays a significant role in the deactivation of the catalysts. Materials like SiO_2, Al_2O_3, MgO, TiO_2, ZrO_2, AlF_3, and modified zeolites can be attacked by the HCl formed in the HDC reaction leading to an increase in surface acidity and/or a decrease in surface area which would exacerbate the effects of both HCl poisoning and coke deposition [26,34–37].

In previous studies [38–41], the gas-phase hydrodechlorination of dichloromethane and chloroform using Pd/C catalysts was investigated, showing high activity (conversion up to 95% for DCM and 100% for TCM were obtained) and high selectivity to non-chlorinated products (higher than 80%). The catalysts were found to be resistant to HCl poisoning and metal sintering under the test conditions, although they underwent significant deactivation due to the irreversible chemisorption of reactants and/or reaction products at the active centers. In a recent paper, Alvarez-Montero et al. [39] presented a comparative study of the behavior of Pd, Ru, Pt, and Rh catalysts supported on activated carbon in the hydrodechlorination of DCM. Under the conditions used in the experiments, the Pt/C catalyst showed, by far, the highest stability, with no sign of deactivation after 65 h on stream. In the current contribution, the performance of the Pt/C catalyst in the gas-phase hydrodechlorination of DCM is investigated in depth. The activity and selectivity of the catalyst are analyzed under different reaction conditions, a reaction scheme is proposed and the value of the activation energy is given. The evolution of its activity and selectivity to non-chlorinated products in very long-term experiments (26 days) is studied and the causes of the high stability of the catalyst are analyzed by means of XPS and TEM. In addition, the performance of the catalyst in the HDC of TCM is also studied.

2. Experimental

2.1. Catalyst preparation

A platinum catalyst supported on a commercial activated carbon was prepared by incipient wetness impregnation using an aqueous solution of $H_2PtCl_6{\cdot}6H_2O$ (Sigma–Aldrich) of appropriate concentration to obtain a nominal Pt loading of 1 wt.%. The activated carbon (described elsewhere [42]) was used with a particle size of 0.25–0.5 mm. Impregnation was followed by overnight drying at room temperature and heating to 100 °C at a rate of 20 °C/h, the final temperature being maintained for 2 h. The activation of the catalyst precursor was carried out by reduction under a continuous flow of H_2 at 250 °C for 2 h. A heating rate of 10 °C/min was used to reach the activation temperature. Hydrogen was supplied by Praxair with a minimum purity of 99.999%.

2.2. Catalyst characterization

The pore structure of the catalyst when fresh and after use in the HDC reaction was characterized from the N_2 adsorption–desorption isotherms at 77 K using a Quantachrome Autosorb 6B apparatus. The samples were previously outgassed for 4 h at 250 °C at a residual pressure of 10^{-3} Torr.

The bulk Pt content was determined via inductively coupled plasma-mass spectroscopy (ICP-MS) in a Perkin-Elmer Elan 6000 Sciex system that was equipped with an autosampler (Perkin-Elmer model AS-91). The samples were previously digested for 15 min in a microwave oven, using a strongly acidic mixture (aqua regia) at 180 °C.

The surface of the catalysts was analyzed by X-ray photoelectron spectroscopy (XPS) with a Physical Electronics 5700C Multitechnique System, using Mg Kα radiation (h_v = 1253.6 eV). To determine all the elements present on the catalyst surface, general spectra were recorded for the samples by scanning the binding energy (BE) from 0 to 1200 eV. The BE of the Pt 4f core level and full width at half maximum (FWHM) values were used to determine the chemical state of Pt. The BE of the Cl 2p peak was used to analyze the chemical state of Cl on the surface of the catalyst. Binding energy values were corrected for the effects of sample charging by taking the C 1*s* peak (284.6 eV) as an internal standard. The accuracy of the BE scale was ±0.1 eV. The data analysis procedure involved smoothing, a Shirley background subtraction, and curve fitting using mixed Gaussian–Lorentzian functions by a least-squares method. The atomic ratios of the elements were calculated from the relative peak areas of the respective core level lines using Wagner sensitivity factors [43].

A Micromeritics ChemiSorb 2705 pulse analyzer was used to measure the dispersion of the fresh and used catalyst by H_2 chemisorption at room temperature. The sample (0.15–0.30 g) was first reduced at 250 °C for 2 h under hydrogen flow and then cooled under helium flow to room temperature. Several pulses of 50 μL H_2 were then introduced until saturation of the catalyst surface was achieved. The number of exposed platinum atoms (Pt_s) was calculated from H_2 chemisorption data (H_{2ads}). The stoichiometry of the adsorption of H_2 on platinum atoms (Pt_s/H_{2ads}) was assumed to be 2 [44–46]. The Supplementary information contains further information on pretreatment of catalyst samples prior to chemisorption and XPS measurements (S1).

Transmission electron microscopy (TEM) analysis was carried out using a JEOL JEM-2100F microscope operating at 200 kV. The instrument had a point resolution of 0.19 nm and was equipped with a high-angle annular dark field (HAADF) detector, a 2 k × 2 k ULTRASCAN 1000 CCD camera, and an Oxford Instruments INCA Energy TEM 250 for chemical analysis by Energy Dispersive X-ray Spectroscopy (XEDS).

High-resolution data were obtained on an aberration corrected FEI-TITAN transmission electron microscope operated at 300 kV with a resolution of 0.08 nm. The STEM images were obtained during periods of 16–20 s using a HAADF detector in order to collect only the high-angle scattered electrons.

For study in the electron microscopes, the samples were dispersed in ethanol and dropped onto holey carbon-coated Cu grids. The characterization of the samples was performed by STEM-HAADF imaging at various magnifications and XEDS for chemical analysis.

2.3. Catalytic activity experiments

The activity of the catalyst for the hydrodechlorination of the chloromethanes was evaluated in a continuous flow reaction system (described elsewhere [38]), consisting essentially of a 9.5 mm i.d. fixed bed micro-reactor coupled to a gas chromatograph with a FID detector for the analysis of the reaction products.

The experiments were performed at atmospheric pressure using a total flow rate of 100 NmL/min and a H_2/chloromethane molar ratio of 100. The gas feed contained a chloromethane concentration of 1000 ppm_v and was prepared by mixing appropriate proportions of a commercial mixture of chloromethane and N_2 with pure N_2. Space–times in the range of τ = 0.08–1.73 kg h mol^{-1} and temperatures of 150–250 °C were employed. To ensure the absence of mass transport limitations, a series of experiments were performed at 250 °C in which the total flow rate and catalyst particle size were varied. No significant changes were found in the chloromethane conversion values at fixed τ values for gas velocity and particle size within the ranges of 0.02–0.06 m/s and 0.25–0.71 mm,

respectively. The behavior of the catalysts was analyzed in terms of the chloromethane conversion (X_A) and selectivities to the different reaction products (S_i). The evolution of the catalytic activity as a function of time on stream was also studied. The carbon mass balance was checked and the closures were found to be 91–98% in DCM experiments and 90–96% for TCM.

The experimental results were reproducible with less than 5% error.

3. Results

3.1. Catalytic activity

3.1.1. Dichloromethane hydrodechlorination

Fig. 1 shows the evolution of DCM conversion (Fig. 1a) and selectivity to the reaction products (Fig. 1b) as a function of space–time at different reaction temperatures over the Pt/C catalyst. Hydrodechlorination of dichloromethane yielded exclusively methane and monochloromethane, with high selectivities to the former in all cases. Dichloromethane conversion showed a significant increase with increasing space–time up to a value of around 0.8 kg h mol^{-1}. Beyond this value, no further significant increase was observed. On the other hand, DCM conversion increased markedly and monotonically with increasing reaction temperature, reaching a value just over 70% at 250 °C for the highest space–time tested. Activation energy (E_a) was calculated from the initial reaction rate values from the Arrhenius plot. A value of E_a = 45.1 kJ/mol with a correlation coefficient of 0.997 was obtained. A similar value of 41.1 kJ/mol was reported by López et al. [16] for the hydrodechlorination of DCM with a Pd/Al_2O_3 catalyst. Lower values in the range 22.1–31.3 kJ/mol were obtained by González Sanchez et al. [24] with Pd/Al_2O_3 and Pd/TiO_2, depending on the Pd content.

Reaction temperature also influenced the selectivity to the reaction products. Increasing the reaction temperature favored the formation of methane to the detriment of monochloromethane, thus reducing the content of chlorinated compounds in the exit stream. In contrast with Pd/C catalysts [41], the formation of hydrocarbons of more than one carbon atom was not favored, even at the highest reaction temperature.

No significant variations in the product distribution were observed with changing space time (Fig. 1b). Methane and monochloromethane were confirmed to be primary products since finite values of selectivity were obtained for both reaction products when extrapolating to zero space–time (Fig. 1b). Moreover, no decrease in MCM selectivity was observed when increasing the space–time. As the dissociative adsorption of the chloromethane reactant is generally accepted for gas-phase hydrodechlorination reactions [11], the formation of methane appears to have taken place exclusively from the adsorbed chloromethyl radical, without desorption of the corresponding intermediate (monochloromethane), by substitution of two chlorine atoms. This probably implies a concerted mechanism as was proposed in previous studies for the hydrodechlorination of TCM and tetrachloromethane (TTCM) with Pd/C catalysts [41,47].

Fig. 2 shows the evolution of DCM conversion as a function of time on stream in a long-term experiment run at a space–time of 0.8 kg h mol^{-1} and at 250 °C. It can be seen that there was no appreciable loss of activity after 26 days of operation. Such long-term stability implies that this catalyst has great potential for industrial application. To the best of our knowledge, catalysts of such stability for the hydrodechlorination of chloromethanes have not previously been reported in the literature. The only reaction products detected were methane and monochloromethane and

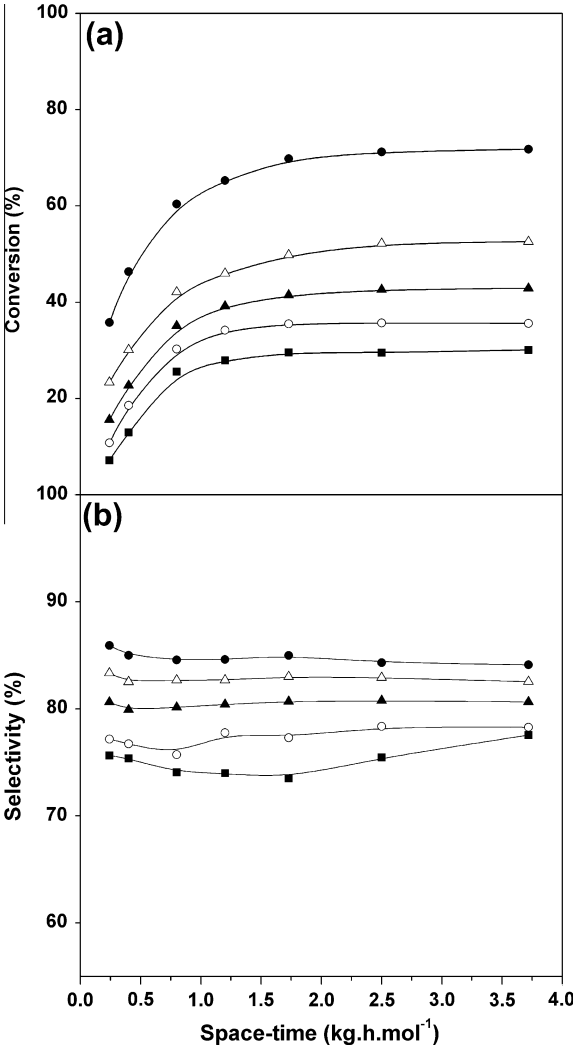

Fig. 1. Effect of space–time on DCM conversion (a) and selectivity to CH_4 (b) in the HDC of DCM with the Pt/C catalyst at different reaction temperatures: (■) 150 °C; (○) 175 °C; (▲) 200 °C; (△) 225 °C; (●) 250 °C.

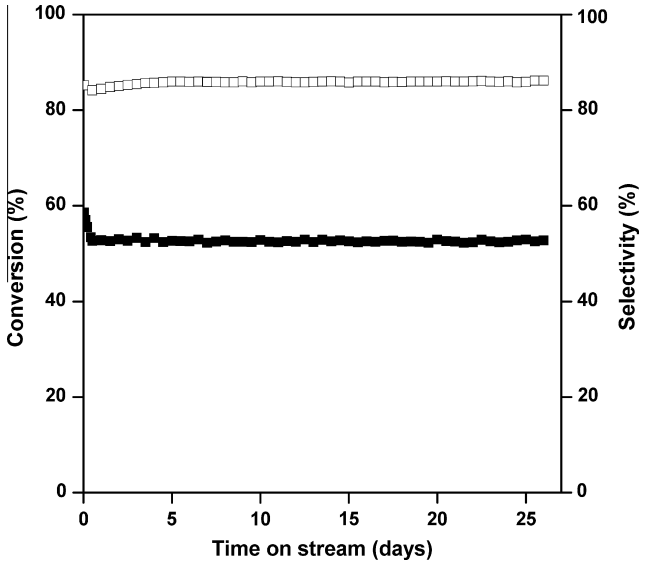

Fig. 2. Evolution of dichloromethane conversion and selectivity to CH_4 with time on stream for the Pt/C at 250 °C and 0.8 kg h mol^{-1} space–time: (■) Conversion; (□) Methane selectivity.

no significant changes in selectivity were detected during the long-term experiment.

3.1.2. Chloroform hydrodechlorination

Table 1 contains values for chloroform conversion and for the selectivity to the reaction products obtained at a space–time of 0.8 kg h mol^{-1} for a reaction temperature range of 125–200 °C. As can be seen, the chloroform was completely converted at 200 °C, a lower temperature than reported for other catalysts [17]. Methane was the only non-chlorinated reaction product detected, unlike in the case of the Pd/C catalysts where the formation of ethane, ethylene, propane, propene, and butane was observed [41]. The selectivity to methane increased with temperature reaching almost 95% at 200 °C. As in the case of the Pd/C catalyst [41], the hydrodechlorination activity was noticeably higher for chloroform than for DCM. A 67% conversion was obtained for chloroform at 125 °C whereas no significant conversion was observed for DCM under the same conditions (for this reason, these low temperature data for DCM are not included in Fig. 1). The differences between the reactivities of these two compounds have been explained by other authors [14] by considering the values of the dissociation energy for the chlorine–carbon bond (325 kJ/mol for TCM and 339 kJ/mol for DCM) [48].

As was found in the hydrodechlorination of DCM, the Pt/C catalyst appeared to be very stable in the HDC of TCM since no deactivation was observed after 167 h on stream at 200 °C and a space–time of 0.08 kg h mol^{-1}. High TCM conversion was obtained with both a substantially lower space–time and a lower temperature than those used for DCM (Fig. 2 and Table 1). Again, no significant changes were found in the selectivity to the reaction products as a function of time on stream.

3.2. Characterization of the catalyst

Table 2 summarizes the BET surface area, pore volume, bulk Pt content, and the Pt dispersion values of the fresh and used catalyst for the hydrodechlorination of DCM (Fig. 2). Both showed a high BET surface area, with fairly similar values of around 1200 m^2/g, which indicates that constriction or partial blockage of the pore structure of the carbon-support did not occur during the reaction at the relatively mild operating conditions.

The fresh catalyst showed a relatively good Pt dispersion (37%) which was similar to that of the Pd/C catalyst reported previously [41]. However, very marked differences were found between the Pt/C and Pd/C catalysts in the evolution of metal dispersion after their use in the HDC reaction. While in the case of the Pd/C catalyst dispersion decreased by more than 75% – from 38% to 9% – [41], a dramatic increase – from 37% to 92% – was observed for the Pt/C catalyst after use under the same conditions.

Table 1
Conversion (X) and selectivity values (S_i) for the HDC of TCM using the Pt/C catalyst at a space–time of 0.8 kg h mol^{-1} and the reaction temperatures (T) indicated.

T (°C)	X (%)	S_{CH_4} (%)	S_{MCM} (%)	S_{DCM} (%)
125	67.0	88.1	4.2	7.7
150	75.1	90.8	4.1	5.1
175	97.8	92.5	3.6	3.9
200	100.0	93.8	3.1	3.1

Table 2
Metal content, BET surface area, and metal dispersion (H_2 chemisorption) of the fresh and used Pt/C catalyst.

Catalyst	Bulk Pt content (wt.%)	S_{BET} (m^2/g)	Pore volume (cm^3/g)	D (%)
Fresh catalyst	0.85	1191	0.52	37
Used catalyst	0.83	1201	0.53	92

The increase in Pt dispersion in the used catalyst is related to a decrease in metal particle size and a better distribution of Pt on the support. Figs. 3 and 4 display the aberration corrected STEM-HAADF images at low magnification (Fig. 3) and at high magnification, with resolution of the atomic columns (Fig. 4), for the fresh and used catalyst. In this mode, only the electrons scattered at very high angle are employed to form the image, and as a consequence, the intensity signal is strongly related to the atomic number of the element analyzed making it very easy to distinguish between heavy elements such as Pt and light atoms such as the carbon of the support. The distributions of Pt particles on the C support in the fresh and used Pt/C catalyst are compared in low magnification images in Fig. 3a and b, respectively. In the fresh sample, the large majority of these particles have unusual elongated shapes. In Fig. 3b, the Pt particles appear significantly smaller and have more spherical morphologies. This confirms the improvement in dispersion of the Pt nanoparticles during time on stream. We propose that the initial elongated particles represent a metastable morphology since at this point the sample had not suffered any high-temperature or otherwise aggressive treatment capable of restructuring the particles and allowing a more energetically stable morphology to occur. This initial elongated shape may be caused by the nature of the solvent evaporation processes or by interactions of the crystalising material with anisotropies in the surface of the carbon-support during impregnation. After prolonged exposure to an aggressive chemical environment at elevated temperatures, however, it is reasonable to expect that the metastable morphology might be replaced by the most thermodynamically stable, spherical shape. This process is indeed observed and appears to be promoted or driven by the attack by Cl-containing species on the elongated Pt particles which results in both the re-dispersion of Pt and the relaxation of the particle morphology to the most stable state (see Supplementary information, S2, for further details).

At higher magnification, Fig. 4a (before reaction) shows a typical, irregularly-shaped, elongated Pt particle of about 4 × 10 nm. Only part of this crystal is in focus, where the atomic distribution can be identified, an effect that is attributed to its formation by the agglomeration of smaller Pt particles with diameters of about 3–7 nm. However, such particles were not observed in the Pt/C catalyst after it was used in the HDC reaction. Fig. 4b and c shows atomic resolution images of two nanoparticles typical of the used catalyst with diameters of 3 and 4 nm, respectively. The mean diameter is slightly smaller than that of the few isolated nanocrystals of the fresh catalyst since particles larger than 5 nm were not observed in the used sample. Fig. 3b shows a Pt nanoparticle orientated in the [1 1 0] zone axis of the *fcc* crystal structure while the Pt particle in Fig. 4c is viewed along the [0 0 1] zone axis (again, related to the *fcc* structure expected for metallic Pt). The morphology of the Pt particles in the used sample is typically close to spherical (although facetted), as would be expected in particles where surface energy relaxation had been allowed to occur. Some atomic vacancies were seen in the nanoparticles, as indicated in Fig. 4c, but these were caused by irradiation in the strong electron beam used in the STEM study. Fig. 5 shows the particle size distributions of the fresh (Fig. 5a) and used (Fig. 5b) catalyst obtained by measuring over a hundred particles for each material. These particle size distributions confirm the decrease in the average metal particle size during the reaction.

The dispersion values in Table 2, the STEM images, and the particle size distribution obtained by this technique (Fig. 5) provide good evidence for the significant re-dispersion of Pt in the Pt/C catalyst during time on stream, even though the average particle size values obtained by the STEM and H_2 chemisorption methods were not coincident (average values of 5.8 and 3.6 nm were obtained for

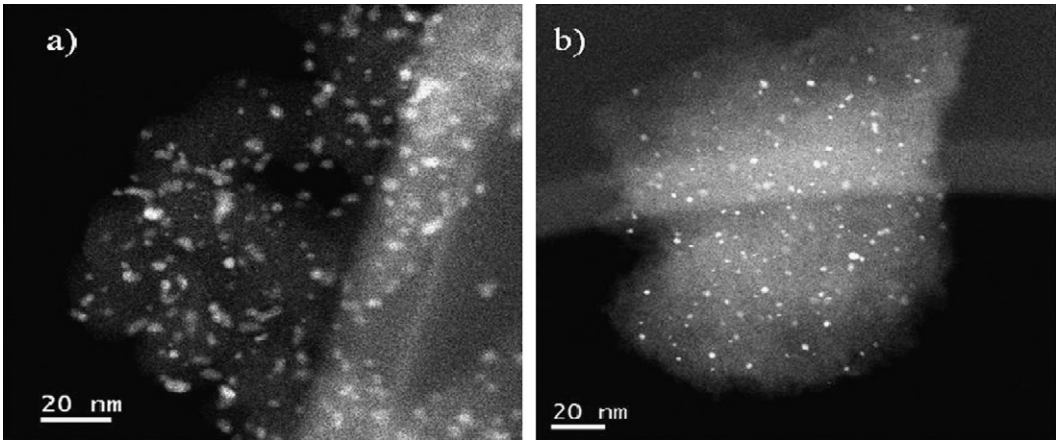

Fig. 3. Cs-corrected STEM-HAADF images of the Pt/C catalyst (a) as-prepared and (b) after use.

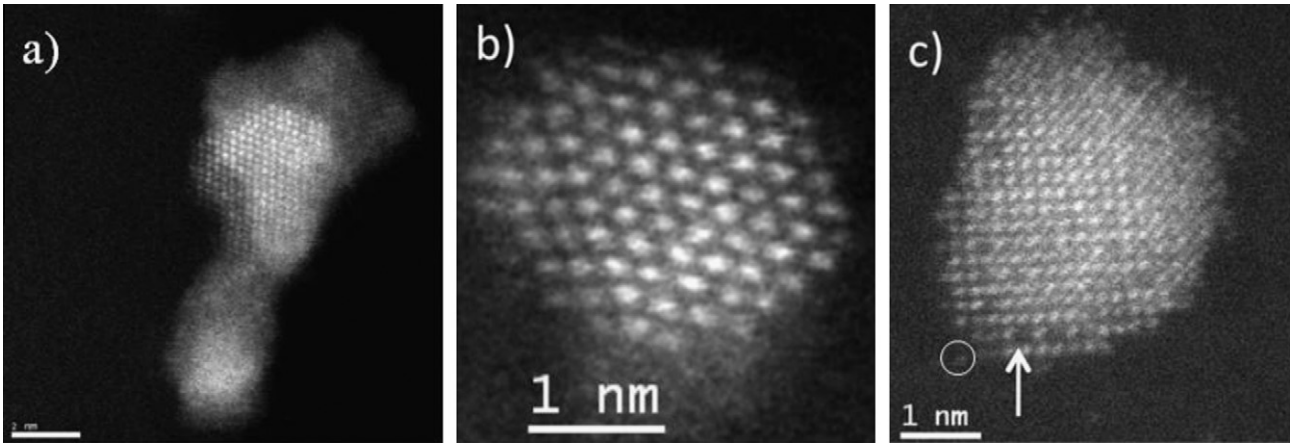

Fig. 4. Cs-corrected STEM-HAADF images of the Pt/C catalyst (a) as-prepared, showing agglomerated nanoparticles; (b) high-resolution image of a Pt nanoparticle in the used catalyst recorded along the [1 1 0] orientation and (c) high-resolution image of a Pt nanoparticle in the used catalyst recorded along the [0 0 1] orientation. The white arrow indicates an atomic vacancy created by the electron beam. An example of features identified as small Pt clusters or single Pt atoms is also circled.

the fresh and used catalyst, respectively, by STEM, while values of 2.9 nm and 1.2 nm, respectively, were obtained by chemisorption). The quantitative identification of very small metal particles by TEM or STEM is not reliable below a certain diameter (approximately <1 nm). Clusters of small particles may also occasionally be identified as single, larger particles. Nevertheless, a dispersion of 92% suggests that a considerable proportion of the Pt was present in clusters of a few atoms and even as single Pt atoms. Indeed, a number of bright features around the particle in Fig. 4c may be interpreted as such structures (marked by a circle in Fig. 4c). These limitations would inevitably give rise to mean particle sizes that were higher than the true value. On the other hand, in certain circumstances, estimation of mean particle sizes from chemisorption data may give slightly smaller values than the true ones. The carbon used as the support in this work is highly microporous and contains a significant proportion of surface functional groups which may allow significant adsorption of H_2 on the carbon-support and so allow spillover of hydrogen species from the Pt particles onto the support. This would exaggerate the specific surface area values obtained and give smaller mean Pt particle size values than the real ones.

Several authors ascribe the re-dispersion of metallic particles to the effect of HCl which they report to provoke the formation, volatilization, and re-deposition of unstable metallic chlorides [26,49]. These chlorides would be reduced in the high concentration of H_2 introduced as a reactant. Ordoñez et al. [26] observed re-dispersion of Pd and Pt in the hydrodechlorination of tetrachloroethylene with commercial catalysts, while in the work of Mori et al. [49] on the hydrodechlorination of CFC-113 with Pd, Pt, Rh, and Ru catalysts, re-dispersion was only observed for Pt. In our case, this phenomenon only occurred with Pt [39]. The stronger interaction of Pd with the carbon-support (as will be explained below) probably disfavors its reaction with the surrounding HCl.

Fig. 6 shows Pt 4f XPS spectra of the Pt/C catalyst as-prepared ("fresh"), after reduction and after use in the HDC of DCM. The band at a binding energy of 72.0 eV for Pt $4f_{7/2}$ corresponds to Pt^0 while the band at around 73.4 eV corresponds to Pt^{n+}. In contrast with the Pd/C catalyst, where similar amounts of electro-deficient (Pd^{n+}) and zero-valent (Pd^0) species were found [38,41], in the reduced fresh Pt catalyst, most of the Pt appears to be in the reduced state (Table 3). On the other hand, the concentration of Pt on the outer surface of the catalyst is closer to the bulk concentration than is the case for Pd in the Pd/C catalyst (Table 3) suggesting than Pt is more homogenously distributed than Pd throughout the catalyst.

The use of acid solutions of Pd chloride for the preparation of the Pd/C catalysts leads to the formation of tetrachloropalladic acid which strongly interacts with the surface of the activated carbon through the adsorption equilibrium $PdCl_4^{2-} + A \leftrightarrow PdCl_{(4-n)^{(2-n)-}}A + nCl^-$. The H^+ and Cl^- remaining on the carbon surface after

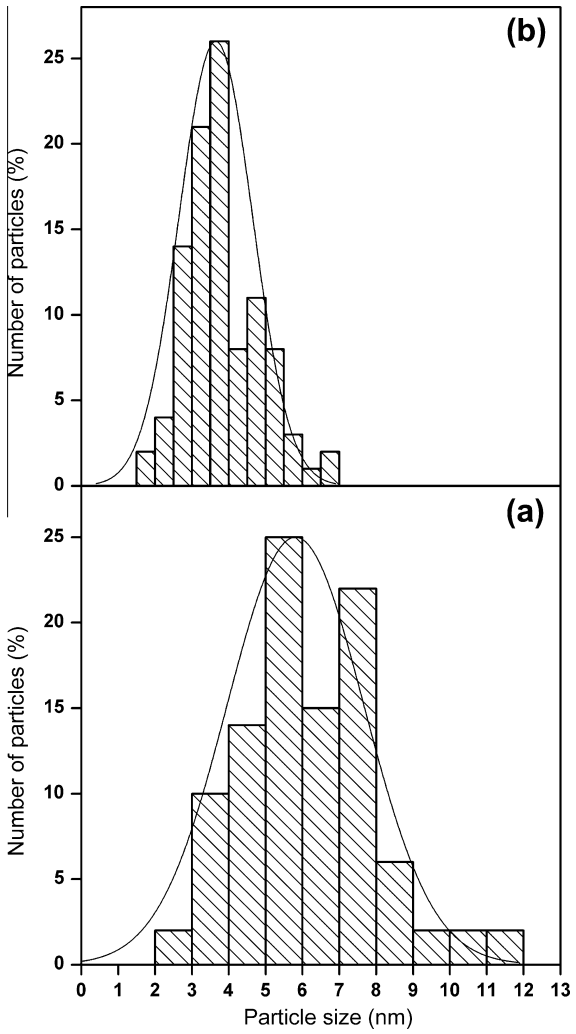

Fig. 5. Metal particle size distribution of Pt/C catalyst obtained by STEM by measuring over a hundred particles for each material: (a) as-prepared and (b) after use.

reduction of the catalyst promote the formation of a significant amount of electro-deficient palladium. The resulting structure is stabilized by the Cl^- ions on the catalyst. This mechanism can be depicted in a simple manner as:

$$Pd^0 + H^+ + Cl^- \rightarrow Pd^{n+} \cdots H^{(1-n)+} \cdots Cl^- \quad (1)$$

According to the mechanism reported in the literature [42,50,51], Pd^{n+} species can be formed in catalysts prepared from H_2PdCl_4, even after careful reduction at about 723 K, by interaction of electron-donating Pd^0 atoms with the neighboring electrophilic protons, which arise from both the tetrachloropalladic acid and the reduction of Pd^{2+}. The small amount of electro-deficient metal species in the as-prepared Pt/C catalyst suggests a weaker interaction of the Pt precursor with the carbon surface.

The Pt 4f XPS spectrum of the used Pt/C catalyst reveals a smaller difference between the relative amounts of zero-valent and electro-deficient Pt than that observed for the reduced fresh catalyst (Table 3): the proportion of electro-deficient Pt increased slightly. In contrast, the proportion of electro-deficient species in the Pd/C catalyst decreased markedly upon use in the HDC process (Table 3).

The Cl 2p XPS spectra of the reduced and used Pt/C catalyst are shown in Fig. 7. Three main bands were observed at binding energies of 198.6, 200.2, and 202.1 eV for the fresh catalyst and 198.0, 200.4, and 202.1 eV for the used one. Binding energies of 198.6 and 198.0 eV correspond to inorganic chlorides while the others correspond to organic chlorides. Whereas the Pd/C catalyst showed a significant increase in the amount of organic chloride (37%) upon use in HDC, no significant corresponding change was found for the Pt/C catalyst (compare results for reduced fresh and used Pt/C catalysts in Table 3). This suggests a greater resistance of this catalyst to poisoning by organochlorine species.

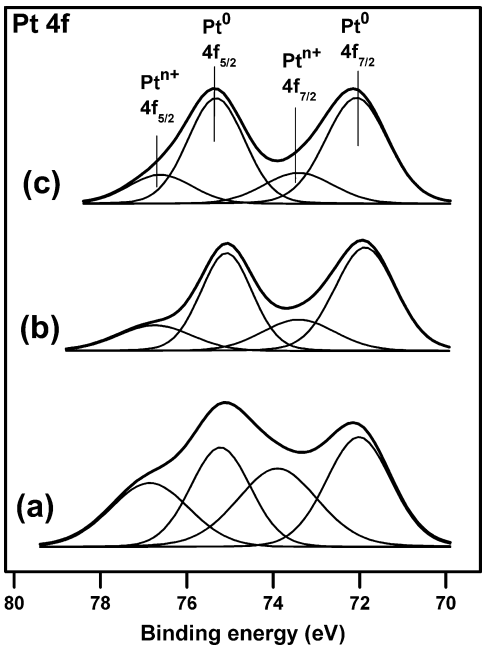

Fig. 6. Pt 4f core level XPS spectra of Pt/C catalyst: (a) fresh unreduced; (b) after reduction in H_2 at 250 °C; (c) after use in the HDC of DCM.

4. Discussion

The Pt/C catalyst was shown to be highly effective for the deep hydrodechlorination of dichloromethane and chloroform. The catalyst has shown a high activity (Fig. 1, Table 1), high selectivity to methane (>80%) and an exceptional stability, with no significant signs of deactivation after 26 days of operation in the hydrodechlorination of DCM.

The overall activity and TOF of the Pt/C catalyst are somewhat lower than those of Pd/C [40]. TOF values of 11,476 h^{-1} and 16,236 h^{-1} were obtained for the Pt/C and Pd/C catalysts, respectively, from the initial reaction rate at a temperature of 250 °C in the HDC of DCM. Further details on the estimation of TOF values are provided in Supplementary information (S3). This can be explained by the higher local density of non-occupied states at the Fermi level, $N(E_f)$, of Pd as a consequence of its specific electronic structure, as has been found in other hydrodechlorination reactions [42,52–54] but also by the larger amount of electro-deficient species in the Pd/C catalyst (Table 3) which is usually reported to improve the activity of these metallic catalysts [55–60]. However, the Pt catalyst also showed a high activity. This can be attributed to the high Pt dispersion on this catalyst and to the more homogeneous distribution of the metallic particles throughout the support (discussed below), as observed by XPS (Table 3) and TEM (Figs. 3–5).

As suggested above, zero-valent Pt (Pt^0) appears to be the main active species in the hydrodechlorination of chloromethanes using the Pt/C catalyst. This interpretation is supported by the high

Table 3
Atomic surface compositions of metal and chloride in the Pt/C and Pd/C catalysts (see text for details).

Catalyst	Me_{XPS} (at.%)	Me^0 (at.%)	Me^{n+} (at.%)	Me_{XPS}/Me_{BULK}	Cl_{XPS} (%)	Cl_{inorg}[a] (%)	Cl_{org}[a] (%)
Pt/C as-prepared	0.06	52.1	47.9	1.1	0.43	37.6	62.4
Pt/C reduced	0.07	74.5	25.5	1.5	0.18	14.9	85.1
Pt/C used	0.04	68.9	31.1	0.8	0.15	13.4	86.6
Pd/C as prepared	0.17	4.5	95.5	1.7	0.57	49.2	50.7
Pd/C reduced	0.32	52.9	47.1	3.3	0.11	46.7	53.3
Pd/C used	0.25	62.3	37.7	2.6	0.13	29.2	70.8

[a] Referred to total chlorine detected by XPS.

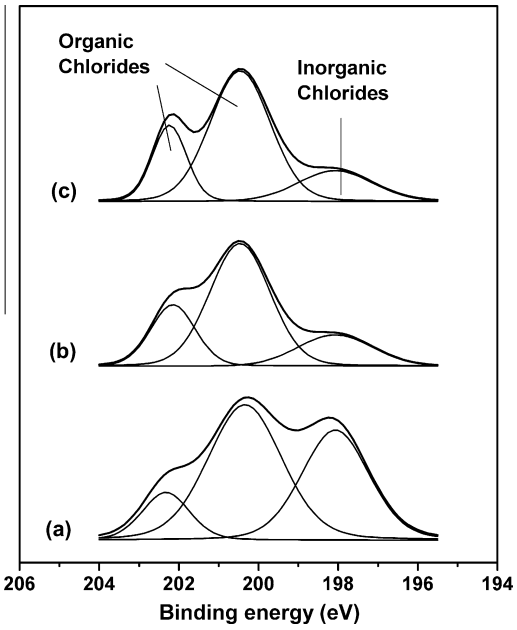

Fig. 7. Cl 2p core level XPS spectra of Pt/C catalyst: (a) fresh unreduced; (b) after reduction in H_2 at 250 °C; (c) after use in the HDC of DCM.

proportion of this species in the Pt/C catalysts (Table 3) and the marked difference observed between the reaction product distributions for the Pd and the Pt catalysts. In contrast with Pd/C, the Pt/C catalyst is not active for the formation of hydrocarbons of more than one carbon atom. This can be partially attributed to the differences in the electronic state of the metal. The formation of higher hydrocarbons than CH_4 seems to be related to the nature of the electro-deficient metal species. In previous work on the hydrodechlorination of chloromethanes using Pd/C catalysts [1,16,32] where the active centers were dual in nature, constituted by the association of neighboring zero-valent and electron-deficient palladium species: $[Pd^0 + Pd^{n+}]$, the chloromethane was found to chemisorb predominantly on the Pd^{n+} sites while hydrogen chemisorbed and homolytically dissociated on Pd^0. On the other hand, the extent of formation of hydrocarbons of more than one carbon atom in the HDC of DCM was considerably lower with a Pd/C catalyst prepared from Pd nitrate, which possessed a smaller proportion of electro-deficient Pd species [41]. In the same way, a wider diversity of hydrocarbons of more than one carbon atom was observed in the HDC of DCM with a Rh/C catalyst which contained a large proportion of Rh in the oxidized state ($Rh^{n+}/Rh^0 \approx 1$ after reduction) [39]. Thus, the formation of hydrocarbons higher than CH_4 seems to require the reaction of two organochloride radicals adsorbed on neighboring electro-deficient metal sites. The low concentration of these sites in the Pt/C catalyst would inhibit the formation of these compounds. Zero-valent Pt (Pt^0) seems to be the main active species for the dissociative adsorption of the chloromethanes in the Pt/C catalyst.

Another important factor which may contribute to the inhibition of the formation of hydrocarbons higher than CH_4 is the high dispersion and homogeneous distribution of Pt particles on the support as revealed by XPS (Table 3) and TEM (Figs. 3–5), which, moreover, improve during the HDC reaction. Re-dispersion of Pt during the reaction leads to very small and homogeneous Pt particles showing very little agglomeration. This probably leads to a higher concentration of H_2 in the vicinity of metallic active centers and higher spillover of H_2, thus favoring the reaction of adsorbed organochloride radicals with the surrounding H_2 and impeding the reaction with other adsorbed organochloride radicals. Other authors have reported a significant influence of metal particle size on the selectivity in other hydrodechlorination reactions with Pd and Pt catalysts [60–62].

The key factor in the performance of the Pt/C catalyst studied here is its high stability. In contrast with the Pd/C catalyst, where significant deactivation was observed with time on stream [38,39,41], no deactivation was observed for Pt/C after 26 days on stream at 250 °C and a space time of 0.8 kg h mol^{-1}. This can be attributed to a greater resistance of the active centers to poisoning by chlorinated hydrocarbons as a consequence of re-dispersion of Pt during the reaction and the different nature of the active metallic species. Re-dispersion of metal particles during the reaction in the Pt/C catalyst, revealed by TEM and H_2 chemisorption, leads to smaller metallic particles with a more homogeneous size distribution, showing very little agglomeration and with a uniform distribution over the support. It is proposed that this uniform distribution could contribute to inhibit the formation and stabilization of chlorocarbons with more than one C atom at the active centers. On the other hand, an increase in conversion would be expected as the dispersion of the active component increased. However, this is not observed here. In fact, the Pt catalyst shows a higher initial activity (Fig. 2). A compensating effect could take place in which the small particles could be intrinsically less active but as the dispersion increases the activity remains very high. The higher initial conversion could be partially due to other phenomena. For example, the adsorption of the reactants on the active centers could be favored by the larger particles and by the higher concentration of Pt in the outer surface of the catalyst, as observed by XPS (Table 3). Further studies are required to gain a deeper understanding of these phenomena. Nevertheless, it seems that a small particle size has a larger positive influence on the selectivity and stability than on the activity.

As explained above, electro-deficient Pd has a higher capacity to stabilize chlorocarbon radicals which may facilitate poisoning by chlorinated hydrocarbons of one or more carbon atoms. This interpretation is supported by the variation of the proportion of zero-valent and electro-deficient species in the used Pd/C and Pt/C catalysts, as determined by XPS. While the proportion of Pd^{n+} decreases significantly in the used Pd/C catalyst – which has been ascribed to poisoning by reactants, intermediates, or reaction products [41] – only a slight decrease in the proportion of Pt^0 was observed in the used Pt/C catalyst. This supports the proposed difference in the nature of the active centers.

It is worth noting that neither carbon deposition nor HCl poisoning is likely to take place in the Pt/C catalyst. Pore blockage is not likely to have occurred, since no significant changes were observed in either the surface area or the pore volume measurements (Table 3). In other studies, where formation of carbonaceous deposits was reported, the surface area and pore volume of the catalyst decreased significantly [26]. In addition, no increase in the surface concentration of inorganic chloride was observed by XPS analysis in the Pt/C catalyst after use in the current study (Table 3).

5. Conclusions

The Pt/C catalyst investigated has been shown to be very efficient for the deep hydrodechlorination of chloromethanes at low concentrations within the temperature range investigated (150–250 °C). It is highly selective to methane, reaching selectivities up to 85% and 93% in the HDC of DCM and of TCM, respectively. The most important feature of the catalyst is its high stability. It showed no significant loss of activity after 26 days on stream in the hydrodechlorination of DCM. The high stability of the Pt/C catalyst can be ascribed to its resistance to coke formation, metal sintering, and poisoning with HCl and organochlorine compounds. The higher resistance to poisoning of these compounds when compared to other catalysts, like Pd/C, can be attributed to redispersion of Pt during the reaction which leads to much smaller metal particles which are very homogeneous in size, show very little agglomeration and are well distributed over the support. It is proposed that these factors would inhibit the formation and stabilization of higher hydrocarbons than CH_4 at the active centers. Moreover, a higher Pt^0/Pt^{n+} ratio favors the stability of the catalyst since Pt^0 appears to be more resistant than Pt^{n+} to poisoning by chloromethane adsorption.

Acknowledgment

The authors gratefully acknowledge financial support from the Spanish MICINN through the project CTM2008-04751. M.A. Álvarez-Montero also wishes to thank the Spanish MEC for her research grant.

Appendix A. Supplementary material

Supplementary data associated with this article can be found, in the online version, at doi:10.1016/j.jcat.2011.02.009.

References

[1] W.J. Hayes, E.R. Laws, Handbook of Pesticide Toxicology, Academic Press, San Diego, 1991.
[2] E. Dobrzynska, M. Posniak, M. Szewczynska, B. Buszewski, Crit. Rev. Anal. Chem. 40 (2010) 41.
[3] N.P. Cheremisinoff, Industrial Solvents Handbook, Marcel Dekker Inc., New York, 2003.
[4] J.V. Michael, K.P. Lim, S.S. Kumaran, J.H. Kiefer, J. Phys. Chem. 97 (1993) 1914.
[5] S.L. Hung, L.D. Pfefferle, Environ. Sci. Technol. 23 (1989) 1085.
[6] H.M. Chiang, J.W. Bozzelli, Combust. Fundam. Appl. Jt. Tech. Meet., Cent. East. States Sect. Combust. Inst. (1993) 322.
[7] J. Rivera, A.A. Barresi, Ingenierías V (2002) 44.
[8] L.N. Zanaveskin, V.A. Aver'yanov, Russ. Chem. Rev. 67 (1998) 713.
[9] L.N. Zanaveskin, V.A. Aver'yanov, Y.A. Treger, Russ. Chem. Rev. 65 (1996) 617.
[10] A. Aizpuru, L. Malhautier, J.C. Roux, J.L. Fanlo, J. Air Waste Manage. Assoc. 51 (2001) 1662.
[11] F.J. Urbano, J.M. Marinas, J. Mol. Catal. A – Chem. 173 (2001) 329.
[12] V.I. Kovalchuk, J.L. d'Itri, Appl. Catal. A – Gen. 271 (2004) 13.
[13] T. Mori, K. Hirose, T. Kikuchi, J. Kubo, Y. Morikawa, J. Jpn. Pet. Inst. 45 (2002) 256.
[14] S. Ordonez, H. Sastre, F.V. Diez, Appl. Catal. B – Environ. 25 (2000) 49.
[15] E. Lopez, S. Ordonez, F.V. Diez, Appl. Catal. B – Environ. 62 (2006) 57.
[16] E. Lopez, S. Ordonez, H. Sastre, F.V. Diez, J. Hazard. Mater. 97 (2003) 281.
[17] L. Prati, M. Rossi, Appl. Catal. B – Environ. 23 (1999) 135.
[18] A. Malinowski, D. Lomot, Z. Karpinski, Appl. Catal. B – Environ. 19 (1998) L79.
[19] T. Mori, T. Kikuchi, J. Kubo, Y. Morikawa, Chem. Lett. (2001) 936.
[20] B. Aristizabal, C.A. Gonzalez, I. Barrio, M. Montes, C.M. de Correa, J. Mol. Catal. A – Chem. 222 (2004) 189.
[21] C.A. Gonzalez, M. Bartoszek, A. Martin, C. Montes de Correa, Ind. Eng. Chem. Res. 48 (2009) 2826.
[22] M. Bonarowska, A. Malinowski, Z. Karpinski, Appl. Catal. A: Gen. 188 (1999) 145.
[23] M. Martino, R. Rosal, H. Sastre, F.V. Díez, Appl. Catal. B – Environ. 20 (1999) 301.
[24] C.A.G. Sanchez, C.O.M. Patino, C. Montes de Correa, Catal. Today 133–135 (2008) 520.
[25] P. Forni, L. Prati, M. Rossi, Appl. Catal. B – Environ. 14 (1997) 49.
[26] S. Ordonez, F.V. Diez, H. Sastre, Appl. Catal. B – Environ. 31 (2001) 113.
[27] B. Heinrichs, F. Noville, J. Schoebrechts, J. Pirard, J. Catal. 220 (2003) 215.
[28] D. Chakraborty, P.P. Kulkarni, V.I. Kovalchuk, J.L. d'Itri, Catal. Today 88 (2004) 169.
[29] M. Legawiec-Jarzyna, A. Srebowata, W. Juszczyk, Z. Karpinski, J. Mol. Catal. A – Chem. 224 (2004) 171.
[30] C. Amorim, G. Yuan, P.M. Patterson, M.A. Keane, J. Catal. 234 (2005) 268.
[31] S. Ordóñez, E. Díaz, R.F. Bueres, E. Asedegbega-Nieto, H. Sastre, J. Catal. 272 (2010) 158.
[32] M. Legawiec-Jarzyna, A. Srebowata, W. Juszykna, Z. Karpinski, Appl. Catal. A – Gen. 271 (2004) 61.
[33] M. Legawiec-Jarzyna, A. Srebowata, W. Juszczyk, Z. Karpinski, React. Kinet. Catal. Lett. 87 (2006) 291.
[34] A.G.F. de Souza, A.M.P. Bentes, A.C.C. Rodrigues, L.E.P. Borges, J.L.F. Monteiro, Catal. Today 107–08 (2005) 493.
[35] B. Coq, J.M. Cognion, F. Figueras, D. Tournigant, J. Catal. 141 (1993) 21.
[36] D. Ju Moon, M. Jo Chung, K. You Park, S. In Hong, Appl. Catal. A – Gen. 168 (1998) 159.
[37] S.Y. Kim, H.C. Choi, O.B. Yanga, K.H. Lee, J.S. Lee, Y.G. Kim, J. Chem. Soc. Chem. Commun. (1995) 2169.
[38] Z.M. de Pedro, L.M. Gomez-Sainero, E. Gonzalez-Serrano, J.J. Rodriguez, Ind. Eng. Chem. Res. 45 (2006) 7760.
[39] M.A. Álvarez-Montero, L.M. Gomez-Sainero, J. Juan-Juan, A. Linares-Solano, J.J. Rodriguez, Chem. Eng. J. 162 (2010) 599.
[40] Z.M. de Pedro, J.A. Casas, L.M. Gomez-Sainero, J.J. Rodriguez, Appl. Catal. B – Environ. 98 (2010) 79.
[41] M.A. Álvarez-Montero, L.M. Gomez-Sainero, M. Martín-Martínez, F. Heras, J.J. Rodriguez, Appl. Catal. B – Environ. 96 (2010) 148.
[42] L.M. Gomez-Sainero, X.L. Seoane, J.L.G. Fierro, A. Arcoya, J. Catal. 209 (2002) 279.
[43] C.D. Wagner, L.E. Davis, M.V. Zeller, J.A. Taylor, R.H. Raymond, L.H. Gale, Surf. Interface Anal. 3 (1981) 211.
[44] F. Coloma, A. SepulvedaEscribano, J.L.G. Fierro, F. RodriguezReinoso, Appl. Catal. A – Gen. 150 (1997) 165.
[45] M.B. Dawidziuk, F. Carrasco-Marin, C. Moreno-Castilla, Carbon 47 (2009) 2679.
[46] C.D. Taboada, J. Batista, A. Pintar, J. Levec, Appl. Catal. B: Environ. 89 (2009) 375.
[47] L.M. Gomez-Sainero, X.L. Seoane, A. Arcoya, Appl. Catal. B – Environ. 53 (2004) 101.
[48] R. Weast, M. Astle, W. Beyer, CRC Handbook of Chemistry and Physics: A Ready-reference Book of Chemical and Physical Data, CRC Press, 1983.
[49] T. Mori, T. Yasuoka, Y. Morikawa, Catal. Today 88 (2004) 111.
[50] N.S. Figoli, P.C. Largentiere, A. Arcoya, X.L. Seoane, J. Catal. 155 (1995) 95.
[51] X.L. Seoane, P.C. Largentiere, N.S. Figoli, A. Arcoya, Catal. Lett. 16 (1992) 137.
[52] P.A. Cox, The Electronic Structure and Chemistry Solids Cap. 3, Oxford Univ. Press, 1987.
[53] R.L. Sproull, Modern Physics: The Quantum Physics of Atoms, Solids and Nuclei, J. Willey & Sons, New York, 1994.
[54] C. Kittel, Introduction to Solid State Physics, J. Wiley, New York, 1986.
[55] N.S. Babu, N. Lingaiah, N. Pasha, J.V. Kumar, P.S.S. Prasad, Catal. Today 141 (2009) 120.
[56] E. Ding, S. Jujjuri, M. Sturgeon, S.G. Shore, M.A. Keane, J. Mol. Catal. A: Chem. 294 (2008) 51.
[57] M.I. Cobo, J.A. Conesa, C.M. de Correa, J. Phys. Chem. A 112 (2008) 8715.
[58] S. Jujjuri, E. Ding, E.L. Hommel, S.G. Shore, M.A. Keane, J. Catal. 239 (2006) 486.
[59] H.C. Choi, S.H. Choi, O.B. Yang, J.S. Lee, K.H. Lee, Y.G. Kim, J. Catal. 161 (1996) 790.
[60] J.W. Bae, I.G. Kim, J.S. Lee, K.H. Lee, E.J. Jang, Appl. Catal. A – Gen. 240 (2003) 129.
[61] S. Gomez-Quero, F. Cardenas-Lizana, M.A. Keane, Ind. Eng. Chem. Res. 47 (2008) 6841.
[62] J.W. Bae, J.S. Lee, K.H. Lee, Appl. Catal. A – Gen. 334 (2008) 156.